

Fully Automatic Electrocardiogram Classification System based on Generative Adversarial Network with Auxiliary Classifier

Zanhong Zhou ¹, Xiaolong Zhai ¹, Chung Tin ¹

ABSTRACT

A generative adversarial network (GAN) based fully automatic electrocardiogram (ECG) arrhythmia classification system with high performance is presented in this paper. We have designed a discriminator (D) to take ECG coupling matrix as input, and then predict the input validity (real or generated) as well as arrhythmia classes. The generator (G) in our GAN is designed to generate various coupling matrix inputs conditioned on different arrhythmia classes for data augmentation. Upon completion of training for our GAN, we extracted the trained D as an arrhythmia classifier in a transfer learning manner. After fine-tuning D by including patient-specific normal beats estimated using an unsupervised algorithm, and generated abnormal beats by G that are usually rare to obtain, our fully automatic system showed superior overall classification performance for both supraventricular ectopic beats (SVEB or S beats) and ventricular ectopic beats (VEB or V beats) on the MIT-BIH arrhythmia database. It surpassed several state-of-art automatic classifiers and can perform on similar levels as some expert-assisted methods. In particular, the F_1 score of SVEB has been improved by up to 12% over the top-performing automatic systems. Moreover, high sensitivity for both SVEB (85%) and VEB (93%) detection has been achieved, which is of great value for practical diagnosis. We, therefore, suggest our ACE-GAN (Generative Adversarial Network with Auxiliary Classifier for Electrocardiogram) based automatic system can be a promising and reliable tool for high throughput clinical screening practice, without any need of manual intervene or expert assisted labeling.

I. INTRODUCTION

Electrocardiogram (ECG) is a clinical standard for diagnosing heart-related diseases, and is particularly valuable for arrhythmia screening and classification. Nevertheless, the interpretation of ECG signal requires extra expertise. Given the large amount of ECG recordings collected in daily clinical routine, interpreting ECG by cardiologists manually is not only resource-exhaustive but also time-consuming. Hence, fully automatic heartbeats classification systems with reliable performance are highly recommended. Various classification systems have been proposed using techniques based on discrete wavelet transform [1], time-domain feature extraction [2], frequency-domain feature extraction [3], feature selection methods [4, 5] and abstract feature [6], etc. Recently, data-driven techniques including convolutional neural network (CNN) which can extract features automatically have started to attract a lot of interests. CNN has shown its strength in various machine learning tasks, including biosignal classification [7, 8] and image recognition [9, 10]. Moreover, it is revealed by previous studies [11-14] that typical CNN based systems can provide superior performance in arrhythmia classification without the need of hand-crafted feature extraction.

Despite the advantages of typical CNNs in arrhythmia diagnosis tasks, they also face several challenges. First, the limited availability of labeled ECG data restricts the performance of typical CNNs, since they are primarily trained in a supervised learning manner. As physiological signals suffer from significant inter-subject variability, previous studies [15-20] have proposed to include some labeled patient-specific heartbeats for boosted classification performance. However, assigning annotations patient by patient would be extremely costly and consequently, those systems are not fully automatic (require expert assistance). Second, the arrhythmic ECG records are intrinsically of imbalanced classes, where normal beats (N beats) commonly outnumber abnormal beats such as supraventricular ectopic beats (SVEB or S beats) and ventricular ectopic beats (VEB or V beats). Some workarounds have been proposed to resolve such a class imbalance problem, including cost-sensitive learning and random re-sampling [21]. However, both random over-sampling and cost-sensitive learning such as assigning different weights to each class [22] could overfit the training data and possibly reduce generalization in actual application. On the other hand, random under-sampling, where a subset of beats can be selected from the overall dataset to fulfill balanced classes [11, 13], would potentially discard important samples and the training set could become too small for training CNN effectively.

¹ Z. H. Zhou (zhzhou7-c@my.cityu.edu.hk), X. L. Zhai (xzhai9-c@my.cityu.edu.hk), and C. Tin (chungtin@cityu.edu.hk) are with Department of Biomedical Engineering, City University of Hong Kong, Hong Kong.

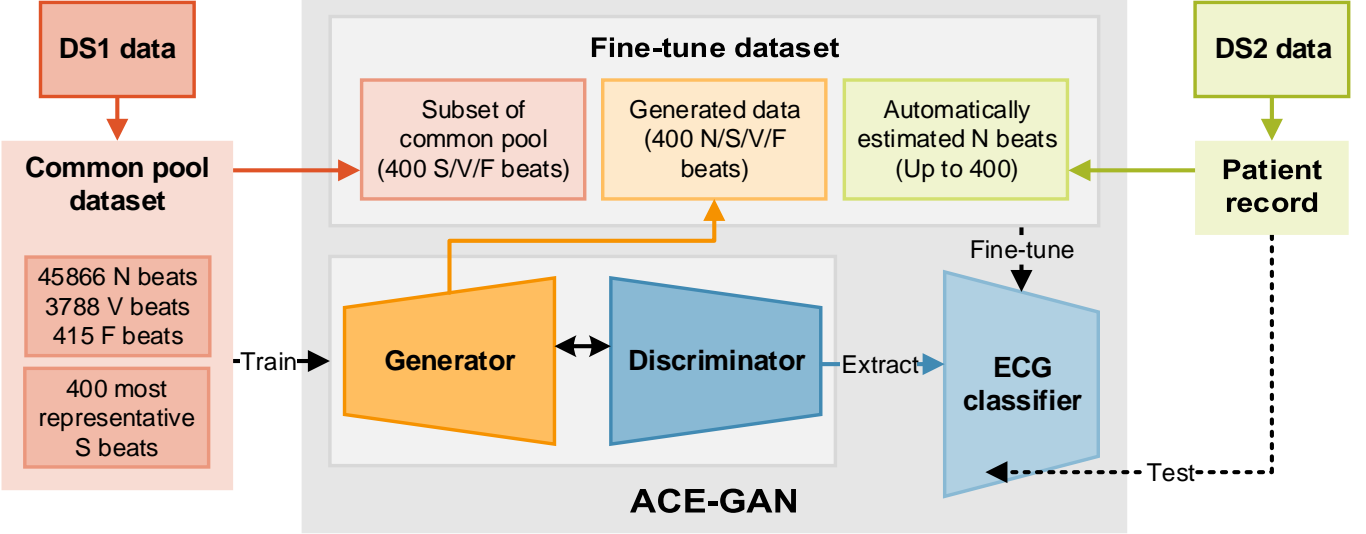


Fig. 1. Schematic of the proposed ACE-GAN based fully automatic arrhythmia classification system. The ACE-GAN is trained with the common pool dataset from DS1. The ECG classifier is extracted from the trained discriminator in a transfer-learning manner and is fine-tuned. The fine-tune dataset comprises of the subset of common pool dataset, the automatically estimated normal beats from the patient, and the generated data from the trained generator as data augmentation. The ECG classifier then serves as the final classifier to predict heartbeat labels for records in DS2.

To tackle the challenges above and meanwhile exploit the benefits of CNN, we suggest that the generative adversarial network (GAN) [23] is a promising approach to overcome these. GAN is a machine learning algorithm and usually contains two neural networks, the generator (G) and the discriminator (D), that can play a zero-sum game, competing and cooperating with each other. In brief, G learns to generate “fake” data that looks like the real one to deceive D ; while D learns to discriminate the fake data generated by G from the real data. As such, GAN has shown great success recently in generating designated data samples through the trained G , such as generating images of specific types from noise [24, 25], transferring images styles [26-28], interpolating high-resolution images [29, 30], and so on. Some studies have also reported the success of GAN in biomedical applications, for example, to de-noise CT images [31] and stain tissue-autofluorescence images [32]. On the other hand, some researchers have looked into the trained D and shown improved performance using it as classifier than traditional deep neural network (DNN) [33-35]. For ECG arrhythmia classification, the GAN may provide data augmentation and relieve class imbalance problem by learning to generate relevant conditional samples.

In this work, we adopted the GAN framework and have designed the ACE-GAN (Generative Adversarial Network with Auxiliary Classifier for ECG) for our ECG arrhythmia classification system. This system includes the G for data augmentation, and extracts the well-trained D for classification in a transfer learning manner. Our system is fully automatic and does not require any manual patient-specific labeling. We tested it on the MIT-BIH arrhythmia database [36, 37] and compared its performance against several previous studies with or without expert assistance following AAMI recommendation [38]. The overall workflow of the proposed systems is summarized in Fig. 1. Details are elaborated in the following sections.

II. DATA PREPARATION

A. Database

To evaluate the performance of the proposed ECG classification systems in this study, we used the publicly accessible MIT-BIH arrhythmia database [36, 37]. This database has been used in numerous previous studies [1, 4-6, 11, 13, 15, 18-20, 22, 39-43] on arrhythmia classification. In this database, 48 ECG recordings from 47 patients are included. Each recording contains two-channel ECG data sampled at 360 Hz for 30 min. Each heartbeat in the record was annotated by at least two cardiologists independently. As defined by AAMI [38], heartbeats in this database can be classified into five types, including N (beats originating in the sinus node), S (supraventricular ectopic beats), V (ventricular ectopic beats), F (fusion beats) and Q (unclassifiable beats). The detailed mapping between MIT-BIH arrhythmia database heartbeat classes and AAMI standard classes is shown in Table I. Four recordings (#102, #104, #107 and #217) that contain paced beats were excluded in this study.

The records in the MIT-BIH database was divided into DS1 and DS2 (Table II), as in many previous studies [4-6, 18-20, 40, 42, 43]. DS1 and DS2 each contain 22 ECG records respectively. DS1 was used as training set while DS2 was regarded as testing set.

TABLE I
Mapping between MIT-BIH Arrhythmia Database Classes and AAMI Classes

AAMI		MIT-BIH Arrhythmia Database	
Classes	Beat Types	Classes	Beat Types
N	Beats originating in the sinus node	• or N	Normal beat
		L	Left bundle branch block beat
		R	Right bundle branch block beat
		e	Atrial escape beat
		j	Nodal (junctional) escape beat
S	Supraventricular ectopic beats	A	Atrial premature beat
		a	Aberrated atrial premature beat
		J	Nodal (junctional) premature beat
		S	Supraventricular premature beat
V	Ventricular ectopic beats	V	Premature ventricular contraction
		E	Ventricular escape beat
F	Fusion beats	F	Fusion of ventricular and normal beat
Q	Unclassifiable beats	/	Paced beat
		f	Fusion of paced and normal beat
		Q	Unclassifiable beat

TABLE II
RECORD NUMBER AND BEATS NUMBER IN DS1 AND DS2

	DS1	DS2	Total
Record #	101, 106, 108, 109, 112, 114, 115, 116, 118, 119, 122, 124, 201, 203, 205, 207, 208, 209, 215, 220, 223, 230	100, 103, 105, 111, 113, 117, 121, 123, 200, 202, 210, 212, 213, 214, 219, 221, 222, 228, 231, 232, 233, 234	-
N	45,866	44,259	90,125
S	944	1,837	2,781
V	3,788	3,221	7,009
F	415	388	803
Q	8	7	15
Total	51,021	49,712	100,733

B. Dual-beat coupling matrix input for classification system

In this study, the modified lead II channel signal was used and the time series ECG signal was preprocessed in a similar way as our previous work [13]. The procedure is briefly repeated here.

For each record in both DS1 and DS2, the segmentation length of one heartbeat is defined as the R-R interval averaged over the whole 30-minute record. Each beat segment is centered on its own R peak. To compute the dual-beat coupling matrix, two pairs of adjacent heartbeats are considered together. The first pair consists of the current beat and the previous beat, denoted as the column vector:

$$\text{Dual_beat}_{i-1,i} = \text{Beat}_{i-1}[1] \dots \text{Beat}_{i-1}[k] \dots \text{Beat}_{i-1}[L], \\ \text{Beat}_i[1] \dots \text{Beat}_i[k] \dots \text{Beat}_i[L] \quad (1)$$

where $\text{Beat}_i[k]$ is the k^{th} sample point of the current beat in time, and L is the original length of beats in this record. The second pair consists of the current beat and the next beat (denoted as the column vector $\text{Dual_beat}_{i,i+1}$ similarly).

These two dual-beat vectors are then scaled respectively to the required input size M as follows. First, the original vector with length $2L$ is interpolated by a factor equals to the input size M . Then, the average values for every $2L$ data points are calculated. As a result, a vector of length M is obtained with any original length of $2L$.

After that, we compute the coupling matrix (CM) with size $M \times M$, as follows,

$$\text{CM} = \begin{bmatrix} \text{Dual_beat}_{i-1,i}^{\text{scaled}}[1] \\ \vdots \\ \text{Dual_beat}_{i-1,i}^{\text{scaled}}[M] \end{bmatrix} \cdot \begin{bmatrix} \text{Dual_beat}_{i,i+1}^{\text{scaled}}[1] & \dots & \text{Dual_beat}_{i,i+1}^{\text{scaled}}[M] \end{bmatrix} \quad (2)$$

The input size M is defined as 73 following our previous work [13]. Our classification system is designed to take this coupling matrix as input and provide a label for the center beat, Beat_i .

C. Common pool dataset

As shown in Fig. 1, our ACE-GAN is trained using the common pool dataset, which includes 50,469 beats (45,866 N beats, 3,788 V beats, 415 F beats, and 400 most representative S beats) in DS1. The 400 S beats, which is close to the number of F beats in the pool, were selected using the iterative method proposed in our previous study [13]. Briefly, a binary classifier (with the same structure as D) is constructed to discriminate N and S beats. Each time, 75 N and 75 S beats were randomly selected from 16 records of DS1 (where S beats exist) to train this classifier. This classifier is then tested on 100 N beats randomly selected from the

remaining 6 records in DS1. This was repeated 200 times using different sets of 75 S beats. After that, we selected the 400 S beats in DS1 that gave the highest average prediction accuracy for N beats in this procedure. These selected S beats are expected to have significantly different morphologies from the N beats and hence should be more useful for the subsequent training [13]. On the other hand, Q beats are not used for training in this study, as these unclassifiable beats are unlikely to help boost classification performance.

D. Fine-tune dataset

Our fine-tune dataset (Fig. 1) comprises of three parts: 1) the 400 most representative S beats as described above, along with 400 V beats and 400 F beats randomly selected from common pool dataset; 2) a new pool of N, S, V and F beats (400 for each class) generated by G (to be elaborated in Section III); and 3) up to 400 automatically estimated N beats as introduced below. All these beats are assigned with a label of “real” beat.

E. Estimation of patient-specific normal beats

Since including patient-specific heartbeats for training can improve performance as introduced [15-20], we here propose a simple unsupervised method to extract N beats from the testing subject reliably. We emphasize that this unsupervised estimation method does not require any manual labeling/intervention, and hence our arrhythmia classification system remains fully automatic.

N beats originating in the sinus node generally have stable and regular rhythms, which can be readily revealed using a simple correlation measure. For each testing recording, we consider the two pairs of dual-beats segments as in computing the coupling matrix. The spectrograms for both dual-beats segments are computed using short-time Fourier Transform (STFT) respectively. We use the 1024-point Fast Fourier Transform (FFT) with a window size of 64 and a step of 1. The spectrogram power is retained only up to 11.23Hz (corresponds to 32 points) where most power of ECG is found. Then, the two spectrograms are unrolled and their correlation coefficient is calculated. A high correlation coefficient (close to 1) generally implies local regularity of the rhythm and the beats are likely to be N beats. Based on this principle, we can use the following algorithm to estimate a number of N beats from each testing record in an unsupervised way:

- 1) For each $Beat_i$, two spectrograms are computed respectively. If the correlation coefficient between them is larger than 0.9, $Beat_i$ will be considered as a normal beat and is stored in the N beat pool (Est_N_Beats).
- 2) If the correlation coefficient is lower than 0.9, the spectrograms will be compared with those calculated from the N beat pool (Est_N_Beats) one by one. If any of the resulting correlation coefficients is larger than a threshold, $Beat_i$ can still be considered as an N beat. The threshold is defined as $0.95 + \text{epoch}/100$. This increasingly stricter criterion helps reduce false positive as the N beat pool (Est_N_Beats) increases in size.
- 3) This procedure is repeated until no more beat is added to the N beat pool (Est_N_Beats) or when the pool size has reached the predefined requirement.

The accuracy of this estimating method for each record in DS2 is shown in Section VI.

III. ACE-GAN

The most important component in our classification system is the ACE-GAN. Fig. 2 presents the architecture of our proposed G and D .

A. Generator architecture

As shown in Fig. 2a, G takes a 100×1 vector of noise ($\sim \mathcal{N}(0,1)$) and a scalar class label as inputs. The label can be any of the four values representing N, S, V or F beat. This scalar is then converted into a 100×1 vector using the embedding function in Keras [44]. The elementwise multiplication of the noise and the embedded label is taken at the first hidden layer of G . This hidden layer further connects to two layers in parallel through full connection, which correspond to the two pairs of adjacent beats required to calculate the coupling matrix (see Section II.B). Batch normalization is deployed before these two layers [45]. Each of these two layers goes through another full connection operation to fit into an input size of 73, and are finally used to compute the coupling matrix as in Eq. 2. We used rectified linear activation units (ReLU) as activation functions for all hidden layers but not the last two layers of G . The second last and the output layer of G are modeled as linear layers such that the magnitudes of the coupling matrix are not limited to ± 1 , in contrast to the commonly used tanh activation. We observed that this allows our G to generate coupling matrices of different classes with higher fidelity for our system.

B. Discriminator architecture

We herein adopted the CNN structure in [13] as our D in this study (Fig. 2b). In brief, it composes of a convolutional layer, a max pooling layer, a second convolutional layer, an average pooling layer and a third convolutional layer with kernel sizes of 8, 2, 10, 3 and 5, respectively. Then a fully connected layer is added in the latter part of this CNN. We again used ReLU as activation functions for these hidden layers. Dropout [46] is applied to the last two layers with a rate of 0.5. In this study, a linear unit is added in parallel to the softmax layer as output, which predicts whether the input comes from the training data or is generated by G .

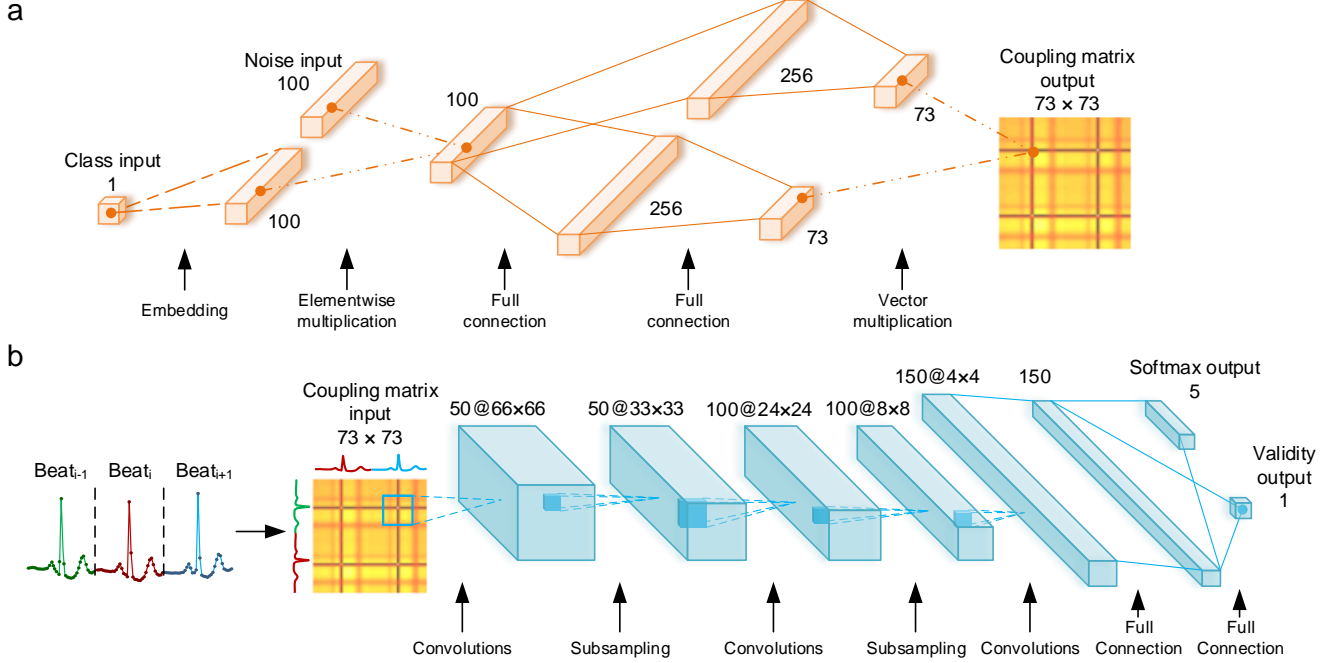


Fig. 2. Schematic of generator architecture (a) and discriminator architecture (b) in the proposed ACE-GAN. The generator takes a 1-dimensional scalar as the designated class label and a 100-dimensional noise vector as inputs. The label scalar is then embedded into a 100-dimensional vector to elementwise multiply with the noise vector input. The output of the generator is one coupling matrix computed by vector multiplication of two 73-dimensional vectors. The discriminator receives the 73 by 73 coupling matrix (computed from 2 pairs of adjacent heartbeat waveforms) as input while outputs a 1-dimensional scalar for validity and a 5-dimensional softmax layer indicating the predicted class label simultaneously. Details are described in Section III.

C. Objective functions and optimization

A variant of GAN named AC-GAN (GAN with auxiliary classifier) has been proposed to generate class-conditional samples [30]. In AC-GAN, G takes random noise input $z \sim p_z$ and class labels $c \sim p_c$ as inputs to generate $\mathcal{X}_{fake} = G(c, z)$. As a result, every generated sample corresponds to a class label and noise input. The D in AC-GAN takes \mathcal{X}_{fake} or $\mathcal{X}_{real} = x \sim p_{data}$ as input, and outputs the probability indicating the chance of the sample coming from a certain source S (real or “fake”), namely $P(S | \mathcal{X})$; as well as the probability of belonging to a certain class C , namely $P(C | \mathcal{X})$ respectively. Therefore, there are two objective functions of concern: \mathcal{L}_S for the likelihood of correct source and \mathcal{L}_C for the likelihood of correct class, as shown below. By training the AC-GAN, D learns to maximize $(\mathcal{L}_C + \mathcal{L}_S)$ while G learns to maximize $(\mathcal{L}_C - \mathcal{L}_S)$.

$$\mathcal{L}_S = E[\log P(S = s_{real} | \mathcal{X}_{real})] + E[\log P(S = s_{fake} | \mathcal{X}_{fake})] \quad (3)$$

$$\mathcal{L}_C = E[\log P(C = c | \mathcal{X}_{real})] + E[\log P(C = c | \mathcal{X}_{fake})] \quad (4)$$

In this work, we designed the ACE-GAN based on AC-GAN with modifications regarding the task of ECG arrhythmia classification. Briefly, G also takes noise $z \sim p_z$ and heartbeat class labels $c \sim p_c$ (i.e. N, S, V or F) as inputs to generate designated dual-beat coupling matrix samples, \mathcal{X}_{fake} . D is trained on both real heartbeat coupling matrices \mathcal{X}_{real} and the generated ones \mathcal{X}_{fake} , in order to predict the validity S as well as the heartbeat class C that \mathcal{X} represents.

Note that in our implementation of D , a real coupling matrix input is expected to be predicted with a validity of 1 at the linear unit (and 0 for a generated input) as well as annotated with a class label indicating the type of beat (N, S, V, F or generated) from the softmax layer. The additional “generated” class label in the softmax layer is included to ensure that D learns to classify beat types only from “real data”. We found that this dual labeling is useful in the training of our ACE-GAN since the samples generated by G in the very early stage of training are far from satisfactory in mimicking the different beat types. Hence, we designed the D to discriminate different beat types only when D has determined it as real beat, which in turn speeds up the learning of G . In addition, we used Mean Square Error (MSE) loss for the objective function of \mathcal{L}_S instead as inspired by LSGAN [47] and Wasserstein distance [48, 49]. This added a penalty to the loss function to describe the distance of distribution between \mathcal{X}_{fake} and \mathcal{X}_{real} . It also helps stabilize the GAN training process, speed up convergence and assist in avoiding mode collapse problems [47].

The objective functions of our proposed ACE-GAN are now modified as follow:

$$\mathcal{L}_S = E[\text{MSE}\{S, s_{real}\} | \mathcal{X}_{real}] + E[\text{MSE}\{S, s_{fake}\} | \mathcal{X}_{fake}] \quad (5)$$

$$\mathcal{L}_C = E[\log P(C = c | \mathcal{X}_{real})] + E[\log P(C = c_{fake} | \mathcal{X}_{fake})] \quad (6)$$

TABLE III
OPERATING ENVIRONMENT AND HYPER-PARAMETERS

Language	Python 3.6.8
Toolbox	Keras 2.2.4 (TensorFlow 1.12.0 backend)
CUDA version	9.2
CUDNN version	7.5
Dropout rate	0.5
BatchNorm momentum	0.8
Number of iterations	10000
Batch size	128
Optimizer	Adam
Learning rate	$\alpha = 0.0001, \beta_1 = 0.5, \beta_2 = 0.999$
Weight initialization	$\mathcal{N}(0, 0.01)$

where D tries to maximize $(\mathcal{L}_C - \mathcal{L}_S)$ while G learns to maximize $(\mathcal{L}_C + \mathcal{L}_S)$.

Both the G and D in our ACE-GAN are randomly initialized from $\sim \mathcal{N}(0, 0.01)$. We used Adam optimizer [50] with a learning rate of 0.0001 for both G and D . Our proposed ACE-GAN is trained for a total of 10000 iterations. In each iteration, G is updated once while D is updated twice (one with real data and one with generated data). The batch size is set to 128. In the training phase of G , a batch of 128×1 randomly assigned labels (including N, S, V, and F) and a 128×100 noise matrix are fed to G to generate coupling matrix samples (\mathcal{X}_{fake}). In the training phase of D , 32 samples from each of the 4 classes (N/S/V/F) are selected randomly from the common pool dataset, resulting in a batch of $32 \times 4 = 128$ training samples (\mathcal{X}_{real}) in total. \mathcal{X}_{fake} is also fed to D with “generated” class label. Through the gradients from D in backpropagation, G learns to generate new coupling matrices from the sampled noise according to these assigned labels. Detailed operating environment and hyper-parameters are shown in Table III.

Upon the training of ACE-GAN using the common pool dataset, the trained D is extracted as the initial ECG classifier and further fine-tuned with the fine-tune dataset (Section II.D). All hyper-parameters for fine-tuning are kept the same as in Table III, except the epoch number. During fine-tuning, the classifier is trained until the classification accuracy has reached 99%, or the absolute change of the accuracy is less than 1% in the last 10 epochs. Then the final classifier is used to predict heartbeat labels for records in DS2.

IV. EVALUATION

We here evaluated the classification performance for S and V beats detection as in several previous studies [5, 11-13, 15, 17, 19, 40-42]. The following five metrics are calculated using the entire 30 min. of the records in DS2, including classification accuracy (Acc), sensitivity (Sen), specificity (Spe), positive predictive rate (Ppr) and F_1 score (F_1):

$$Acc = \frac{TP+TN}{TP+TN+FP+FN} \quad (7)$$

$$Sen = \frac{TP}{TP+FN} \quad (8)$$

$$Spe = \frac{TN}{TN+FP} \quad (9)$$

$$Ppr = \frac{TP}{TP+FP} \quad (10)$$

$$F_1 = 2 \cdot \frac{Sen \cdot Ppr}{Sen + Ppr} \quad (11)$$

where TP is the true positive, TN is the true negative, FP is the false positive and FN is the false negative.

V. RESULTS

The performance of our ACE-GAN is evaluated and the results are summarized in Table IV. The simulations are repeated 10 times where G generates different random input samples. The performance of the classifier remains quite stable with small variations. The corresponding confusion matrix of our proposed system is shown in Table V. In confusion matrices listed in this study, the “generated” class represents heartbeats that our classifiers considered as fake/generated, probably due to their low fidelity or unprecedented abnormality. These beats are regarded as misclassification in our analysis.

Our fully automatic system achieves very high Acc and Spe for both SVEB (99% and 99% respectively) and VEB (99% and 99% respectively), which are comparable with several state-of-art studies (Table IV). More importantly, the Sen for SVEB (85%) and VEB (93%) in our system are higher than those of all previous automatic systems under comparison [4, 5, 19, 20, 40, 42, 43, 51]. In fact, the Sen for SVEB and VEB of our system are comparable with some of the expert assisted systems, which require manual annotation for up to 500 beats or 5 minutes of ECG recording for each testing subject (Table IV). Such high Sen is important for practical clinical use. Furthermore, our Ppr of SVEB indeed ranks second among all these automatic methods compared, while Ppr of VEB is quite high at 90%. Consequently, relatively high F_1 scores for both VEB (91%) and SVEB (85%) are achieved. Actually, our F_1 scores for SVEB is higher than the top-ranked automatic method in Table IV by up to 12%.

TABLE IV
SVEB AND VEB CLASSIFICATION PERFORMANCE OF THE PROPOSED SYSTEMS AND COMPARISON WITH FORMER STUDIES (22 TESTING RECORDS IN DS2)

	Fully automatic	# labels required / patient	SVEB (%)					VEB (%)				
			Acc	Sen	Spe	Ppr	F ₁	Acc	Sen	Spe	Ppr	F ₁
Automatic systems												
Mar <i>et al.</i> [5]	Yes	-	93.3	83.2	93.7	33.5	47.8	97.4	86.8	98.1	75.9	81.0
Zhang <i>et al.</i> [42]			93.3	79.1	93.9	36.0	49.5	98.6	85.5	99.5	92.7	89.0
Chazal <i>et al.</i> [40]			94.6	75.9	95.4	38.5	55.1	97.4	77.7	98.8	81.9	79.7
Llamedo & Martínez [4]			95.1	76.5	95.8	41.3	53.6	98.2	83.1	99.2	88.1	85.5
Garcia <i>et al.</i> [51]			96.6	62.0	97.9	53.0	57.1	95.4	87.3	95.9	59.4	70.7
Llamedo & Martínez [19]			-	79 ± 2	-	46 ± 2	58.1	-	89 ± 1	-	87 ± 1	88.0
Raj & Ray [43]			96.2	80.8	96.7	48.8	60.8	97.9	82.2	99.0	85.4	83.8
Ye <i>et al.</i> [20]			98.3	61.4	99.8	90.7	73.2	99.4	91.8	99.9	98.3	94.9
Proposed ACE-GAN			99 ± 0	85 ± 2	99 ± 0	85 ± 2	85 ± 1	99 ± 0	93 ± 1	99 ± 0	90 ± 1	91 ± 1
Expert assisted systems												
Chazal & Reilly [18]	No	500 beats	95.8	87.7	96.1	47.0	61.2	99.4	94.3	99.7	96.2	95.2
Llamedo & Martínez [19]		1 beat	-	83 ± 4	-	58 ± 5	68.3	-	91 ± 3	-	90 ± 2	90.5
Chazal [17]		100 beats	97.8	94.0	-	62.5	75.1	99.4	93.4	-	97.0	95.2
Ye <i>et al.</i> [20]		5 min.	99.1	76.5	99.9	99.1	86.3	99.7	97.1	99.9	98.5	97.8
Llamedo & Martínez [19]		12 beats	-	92 ± 1	-	90 ± 3	91.0	-	93 ± 1	-	97 ± 1	95.0

TABLE V
CONFUSION MATRIX FOR THE PROPOSED ACE-GAN BASED
FULLY AUTOMATIC SYSTEM TESTING ON DS2

	N	S	V	F	Q	Generated
N	43613	228	207	98	0	113
S	180	1582	64	1	0	10
V	141	44	2989	43	0	4
F	258	0	30	100	0	0
Q	3	0	4	0	0	0

VI. DISCUSSION

In this study, we have proposed an ECG classifier (D) based on a GAN framework to achieve desirable performance.

To examine how the D contributes to ECG arrhythmia classifications, we have performed further simulations. Fig. 3 shows the performance of our system with or without using the extracted D , when fine-tuned with different numbers of generated samples from G , respectively. In the case without the extracted D , another classifier with the same structure as D but with randomly initialized weights is used (referred to as the “fresh classifier” in the following discussion). The fresh classifier is trained on the same fine-tune dataset (see Section II.D) as we fine-tune the extracted D . All training conditions for both classifiers remain the same. Fig. 3 illustrates that using the extracted D can boost the overall classification performance by around 20% for the F_1 of SVEB (Fig. 3a) and around 5% for that of VEB (Fig. 3d). In particular, the Ppr of SVEB is improved dramatically by over 25% (Fig. 3c). For VEB, a 5% increase can also be observed for both Sen (Fig. 3e) and Ppr (Fig. 3f). Therefore, it suggests that the extracted D possesses richer information favorable to arrhythmia detection than the fresh classifier, which could come from its interplay with numerous generated samples from G and the whole common pool dataset throughout the training. The fresh classifier has higher Sen of SVEB than the one using trained weights from D (Fig. 3b). However, it comes at a cost of very low Ppr of SVEB (<40%, Fig. 3c) and consequently, low F_1 of SVEB (<55%, Fig. 3a) which is inappropriate for real world application.

Fig. 3 also shows the effect of different numbers of generated samples per class on the classification performance. Generally speaking, the generated beats mildly improve the performance (by ~5%) in the case of using extracted D . However, when too many generated samples are used (>400), the Sen increases at the cost of declining Ppr. A compromise between Sen and Ppr, hence, needs to be considered. The effects of generated samples are much larger in the case of using the fresh classifier. On one hand, it implies that the trained D has already possessed significant information distribution of generated samples from G , as compared to a fresh network. Hence, providing more generated samples to the trained D has minor effect to improve its classification performance. On the other hand, this also suggests that the trained G indeed is capable of generated meaningful samples through the GAN framework. Fig. 4 presents some examples of generated coupling matrices from different beat types alongside their real counterparts with similar patterns. For instance, the generated coupling matrix for N beat (Fig. 4e) has a regular rhythm like the real one (Fig. 4a) but with different R-R intervals and baseline levels. The generated matrices for abnormal beats (Fig. 4f-h) show irregular rhythm similar to their real counterparts (Fig. 4b-d). Hence, our trained G is not merely making replicates of heartbeats from a known record in a single patient, but is able to generate meaningful samples with variation from the training data which may mimic the inputs for unseen patients. Essentially, the construction of our coupling matrix input using a pair of adjacent heartbeat segments could be regarded as a 2nd order polynomial feature transform, which is a simple and commonly used approach for seeking linearly separable features in higher-dimensional space. However, our coupling matrix is also geometrically structured to preserve physiological information, which is preferable for CNN to extract features automatically.

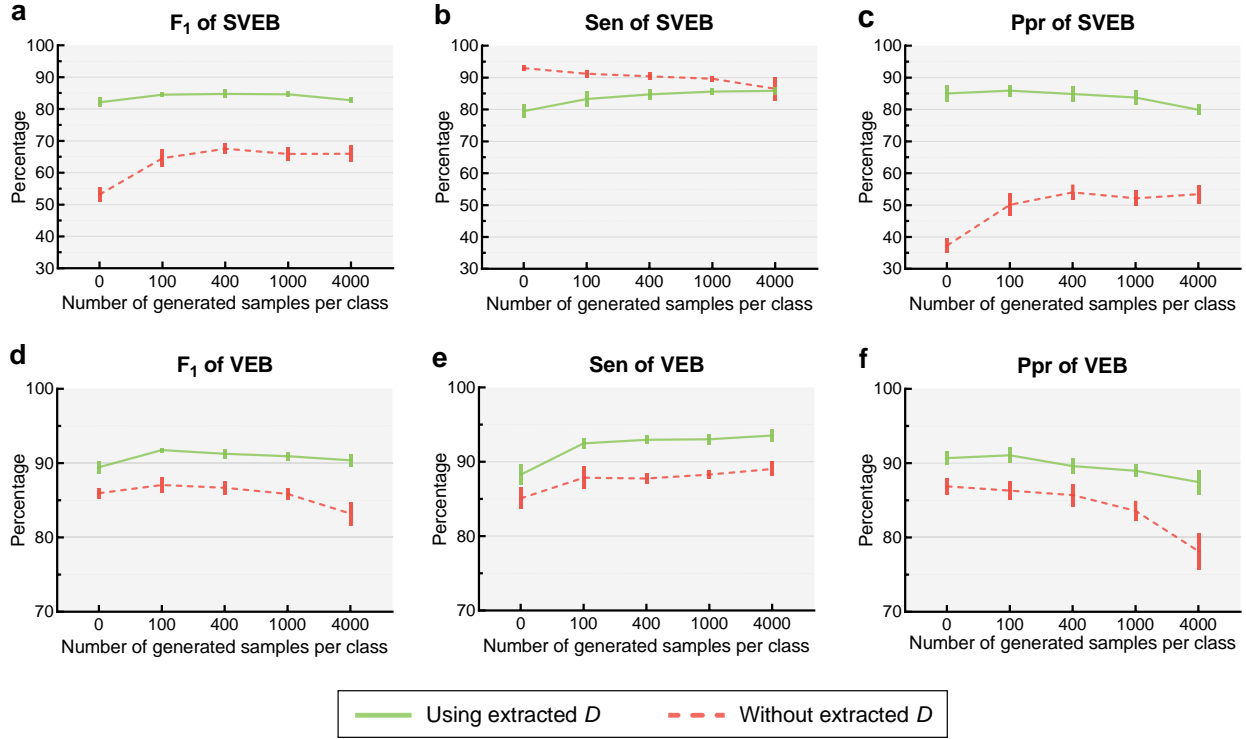


Fig. 3. Comparison of performance with or without using the weights from the trained D , when including different numbers of generated samples from G in the fine-tune dataset. Green: the trained D is extracted to initialize the ECG classifier; Red: the ECG classifier is randomly initialized. Error bars show standard derivation. All classifiers are fine-tuned with the fine-tune dataset, which includes the subset of common pool dataset, the automatically estimated N beats, and 0-4000 generated samples per class.

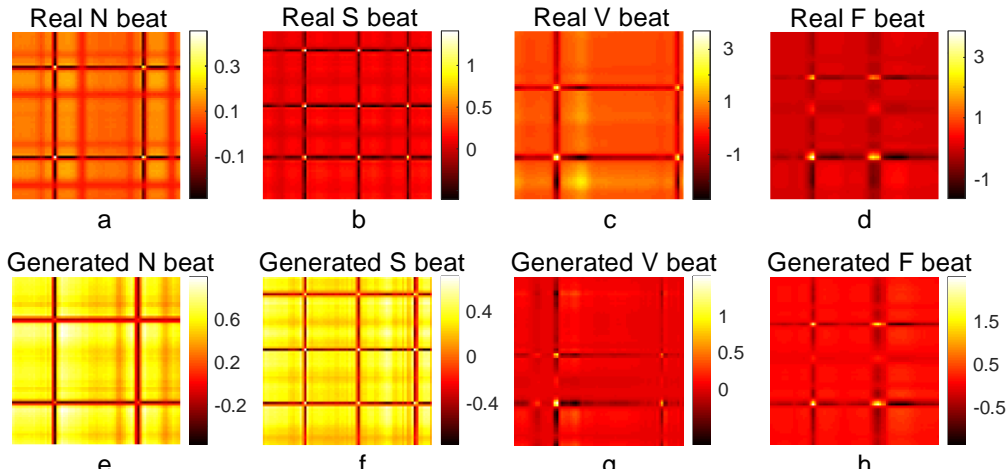


Fig. 4. Representative examples of real coupling matrices among N, S, V and F beats (a-d) and their comparable generated counterparts (e-h).

In our system, the fine-tuning step serves three purposes. First, Table VI shows that without any fine-tuning, the extracted D labeled a number of beats as generated from G , probably because the trained D can only marginally discriminate real and generated samples. Hence, during the fine-tuning step, all training inputs are considered as “real” samples, in order to push the final classifier to predict the type of beats, regardless of the source (real or generated). As a result, the number of beats predicted as “generated” is much reduced as shown in Table V and Tables VII-VIII. Second, fine-tuning with additional beats from G serves a data augmentation purpose to improve the performance (Fig. 3). However, apparently, the role of G for data augmentation seems to contribute more during the training of the GAN. The iterative training of G and D has fed D with numerous generated samples with progressively improving quality. Third, fine-tuning with the subject-specific estimated N beats turns the classifier into a patient-dependent classifier. It significantly increases the Ppr of SVEB (47% to 85%), and consequently, the corresponding F_1

TABLE VI
CONFUSION MATRIX FOR THE EXTRACTED *D* TESTING DIRECTLY ON DS2 WITHOUT FINE-TUNING

	N	S	V	F	Q	Generated
N	26581	1080	184	845	0	15569
S	101	286	27	1	0	1422
V	199	13	1843	19	0	1147
F	231	0	29	32	0	96
Q	2	0	1	0	0	4

TABLE VII
CONFUSION MATRIX FOR THE EXTRACTED *D* FINE-TUNED
WITHOUT GENERATED SAMPLES

	N	S	V	F	Q	Generated
N	42550	237	216	147	0	1109
S	139	1519	44	0	0	135
V	196	23	2869	52	0	81
F	317	0	22	48	0	1
Q	2	0	3	0	0	2

TABLE VIII
CONFUSION MATRIX FOR THE EXTRACTED *D* FINE-TUNED
WITHOUT COMMON POOL DATA

	N	S	V	F	Q	Generated
N	42548	389	887	133	0	302
S	122	1606	101	0	0	8
V	142	29	3025	21	0	4
F	284	2	40	62	0	0
Q	2	0	5	0	0	0

TABLE IX
PERFORMANCE OF THE PROPOSED CLASSIFICATION SYSTEM WITH DIFFERENT COMPONENTS OF FINE-TUNE DATASET

	Fine-tune dataset			SVEB (%)				VEB (%)					
	Estimated N beats	Sub-set of common pool	Generated samples	Acc	Sen	Spe	Ppr	F_1	Acc	Sen	Spe	Ppr	F_1
a)	✓	✓	✗	99 ± 0	79 ± 2	99 ± 0	85 ± 3	82 ± 1	99 ± 0	88 ± 1	99 ± 0	91 ± 1	89 ± 1
b)	✓	✗	✓	99 ± 0	88 ± 1	99 ± 0	76 ± 2	81 ± 1	97 ± 0	93 ± 1	98 ± 0	73 ± 1	82 ± 1
c)	✗	✓	✓	96 ± 0	80 ± 2	97 ± 0	47 ± 2	59 ± 2	99 ± 0	92 ± 1	99 ± 0	87 ± 2	89 ± 1

a) Equivalent to Fig. 3 using extracted *D* with 0 generated samples. Representative confusion matrix listed in Table VII.

b) 400 S/V/F beats per class are generated. Representative confusion matrix listed in Table VIII.

c) The estimated N beats are replaced with 400 N beats selected randomly from the common pool dataset.

TABLE X
ACCURACY OF N BEATS ESTIMATION FROM 22 TESTING RECORDS IN DS2

Record	Correct number	Incorrect number	Accuracy	Record	Correct number	Incorrect number	Accuracy
100	400	0	100.0%	212	400	0	100.0%
103	400	0	100.0%	213	387	13	96.8%
105	400	0	100.0%	214	400	0	100.0%
111	400	0	100.0%	219	395	5	98.8%
113	400	0	100.0%	221	400	0	100.0%
117	400	0	100.0%	222	231	0	100.0%
121	400	0	100.0%	228	106	0	100.0%
123	400	0	100.0%	231	400	0	100.0%
200	29	0	100.0%	232	-	-	-
202	400	0	100.0%	233	400	0	100.0%
210	400	0	100.0%	234	400	0	100.0%
				Avg.	343	1	99.7%

score has also been improved from 59% to 85% (Tables IV and IX). The performance of VEB detection also improves slightly. This indicates that these estimated N beats are useful for arrhythmia detection. We also point out that these subject-specific N beats can be reliably extracted in an unsupervised way, hence allowing the system to remain fully automatic. Table X presents the accuracy of the proposed N beats estimation method for each patient in DS2. Up to 400 N beats were estimated for each patient. The overall accuracy for estimating N beats is 99.7%, which is significantly higher than the chance level of 89.0% in DS2. Note that 100% accuracy has been achieved in 19 out of 22 patients in DS2. No N beat could be estimated from #232 because sinus bradycardia occupied the whole 30min recording and there were numerous long pauses up to 6 sec such that regular rhythm was difficult to detect. It is shown that combining the common pool, the generated samples and the estimate N beats achieves the best overall performance (Tables IV and IX).

Table IV indicates that our proposed system clearly has superior performance in SVEB prediction than all the automatic systems on the list, except for the Ppr in Ye *et al.* [20]. They proposed a subject-adaptable ECG classifier based on a multi-view learning framework. A few high-confidence beats were selected from the testing subject's record, based on labels given by preliminary classifiers that trained with common set data. They also selected some training samples with similar N beat pattern as the testing subject's, and 50-150 representative S or V beats to be included in the training data. By integrating the prediction by both the general model and the specific model, their automatic system achieved a very high Ppr of SVEB (90.7%) and VEB (98.3%). However, both their automatic system and expert assisted system suffered from a relatively low Sen of SVEB (61.4% and 76.5%), as shown in Table. IV, which greatly limits the viability of practical clinical usage.

VII. CONCLUSION

In this study, we have proposed a fully automatic arrhythmia classification system based on our designed ACE-GAN. Its performance in detection for SVEB and VEB outperforms several state-of-art automatic systems and also some expert assisted methods. We have also performed detailed simulations to present the contribution of each component in our system. This work reveals the effectiveness of GAN based systems in ECG classification, and the potential of our proposed system as a promising tool for clinical arrhythmic beats screening.

REFERENCE

- [1] C. Ye *et al.*, "Heartbeat Classification Using Morphological and Dynamic Features of ECG Signals," *IEEE Transactions on Biomedical Engineering*, vol. 59, no. 10, pp. 2930-2941, 2012.
- [2] E. B. Mazomenos *et al.*, "A Time-Domain Morphology and Gradient based algorithm for ECG feature extraction," in *2012 IEEE International Conference on Industrial Technology*, 2012, pp. 117-122.
- [3] I. Romero, and L. Serrano, "ECG frequency domain features extraction: a new characteristic for arrhythmias classification," in *2001 Conference Proceedings of the 23rd Annual International Conference of the IEEE Engineering in Medicine and Biology Society*, 2001, pp. 2006-2008 vol.2.
- [4] M. Llamedo, and J. P. Martinez, "Heartbeat Classification Using Feature Selection Driven by Database Generalization Criteria," *IEEE Transactions on Biomedical Engineering*, vol. 58, no. 3, pp. 616-625, 2011.
- [5] T. Mar *et al.*, "Optimization of ECG Classification by Means of Feature Selection," *IEEE Transactions on Biomedical Engineering*, vol. 58, no. 8, pp. 2168-2177, 2011.
- [6] T. Teijeiro *et al.*, "Heartbeat Classification Using Abstract Features From the Abductive Interpretation of the ECG," *IEEE Journal of Biomedical and Health Informatics*, vol. 22, no. 2, pp. 409-420, 2018.
- [7] X. Zhai *et al.*, "Self-Recalibrating Surface EMG Pattern Recognition for Neuroprosthesis Control Based on Convolutional Neural Network," *Frontiers in Neuroscience*, vol. 11, 2017.
- [8] O. Ronneberger *et al.*, "U-Net: Convolutional Networks for Biomedical Image Segmentation," in *Medical Image Computing and Computer-Assisted Intervention – MICCAI 2015*, 2015, pp. 234-241.
- [9] A. Krizhevsky *et al.*, "ImageNet Classification with Deep Convolutional Neural Networks," *Advances in Neural Information Processing Systems 25*, pp. 1097-1105: Curran Associates, Inc., 2012.
- [10] K. Simonyan, and A. Zisserman, "Very Deep Convolutional Networks for Large-Scale Image Recognition," *arXiv:1409.1556 [cs]*, 2014.
- [11] S. Kiranyaz *et al.*, "Real-Time Patient-Specific ECG Classification by 1-D Convolutional Neural Networks," *IEEE Transactions on Biomedical Engineering*, vol. 63, no. 3, pp. 664-675, 2016.
- [12] U. R. Acharya *et al.*, "Automated detection of arrhythmias using different intervals of tachycardia ECG segments with convolutional neural network," *Information Sciences*, vol. 405, pp. 81-90, 2017.
- [13] X. Zhai, and C. Tin, "Automated ECG Classification Using Dual Heartbeat Coupling Based on Convolutional Neural Network," *IEEE Access*, vol. 6, pp. 27465-27472, 2018.
- [14] A. Y. Hannun *et al.*, "Cardiologist-level arrhythmia detection and classification in ambulatory electrocardiograms using a deep neural network," *Nature Medicine*, vol. 25, no. 1, pp. 65-69, 2019.
- [15] M. M. A. Rahhal *et al.*, "Deep learning approach for active classification of electrocardiogram signals," *Information Sciences*, vol. 345, pp. 340-354, 2016.
- [16] Y. Xia *et al.*, "An Automatic Cardiac Arrhythmia Classification System With Wearable Electrocardiogram," *IEEE Access*, vol. 6, pp. 16529-16538, 2018.
- [17] P. d. Chazal, "An adapting system for heartbeat classification minimising user input," in *2014 36th Annual International Conference of the IEEE Engineering in Medicine and Biology Society*, 2014, pp. 82-85.
- [18] P. d. Chazal, and R. B. Reilly, "A Patient-Adapting Heartbeat Classifier Using ECG Morphology and Heartbeat Interval Features," *IEEE Transactions on Biomedical Engineering*, vol. 53, no. 12, pp. 2535-2543, 2006.
- [19] M. Llamedo, and J. P. Martinez, "An Automatic Patient-Adapted ECG Heartbeat Classifier Allowing Expert Assistance," *IEEE Transactions on Biomedical Engineering*, vol. 59, no. 8, pp. 2312-2320, 2012.
- [20] C. Ye *et al.*, "An Automatic Subject-Adaptable Heartbeat Classifier Based on Multiview Learning," *IEEE Journal of Biomedical and Health Informatics*, vol. 20, no. 6, pp. 1485-1492, 2016.
- [21] N. V. Chawla *et al.*, "Editorial: special issue on learning from imbalanced data sets," *SIGKDD Explor. Newsl.*, vol. 6, no. 1, pp. 1-6, 2004.
- [22] S. S. Xu *et al.*, "Towards End-to-End ECG Classification with Raw Signal Extraction and Deep Neural Networks," *IEEE Journal of Biomedical and Health Informatics*, pp. 1-1, 2018.
- [23] I. J. Goodfellow *et al.*, "Generative adversarial nets," in *Proceedings of the 27th International Conference on Neural Information Processing Systems - Volume 2*, 2014, pp. 2672-2680.
- [24] M. Mirza, and S. Osindero, "Conditional Generative Adversarial Nets," *arXiv e-prints*, 2014.
- [25] S. Reed *et al.*, "Generative Adversarial Text to Image Synthesis," in *Proceedings of The 33rd International Conference on Machine Learning*, 2016, pp. 1060--1069.
- [26] X. Chen *et al.*, "InfoGAN: interpretable representation learning by information maximizing generative adversarial nets," in *Proceedings of the 30th International Conference on Neural Information Processing Systems*, 2016, pp. 2180-2188.
- [27] J.-Y. Zhu *et al.*, "Unpaired Image-to-Image Translation using Cycle-Consistent Adversarial Networks," *arXiv e-prints*, 2017.
- [28] P. Isola *et al.*, "Image-to-Image Translation with Conditional Adversarial Networks," *arXiv e-prints*, 2016.
- [29] C. Ledig *et al.*, "Photo-Realistic Single Image Super-Resolution Using a Generative Adversarial Network," *arXiv e-prints*, 2016.

[30] A. Odena *et al.*, "Conditional image synthesis with auxiliary classifier GANs," in *Proceedings of the 34th International Conference on Machine Learning - Volume 70*, 2017, pp. 2642-2651.

[31] J. M. Wolterink *et al.*, "Generative Adversarial Networks for Noise Reduction in Low-Dose CT," *IEEE Transactions on Medical Imaging*, vol. 36, no. 12, pp. 2536-2545, 2017.

[32] Y. Rivenson *et al.*, "Virtual histological staining of unlabelled tissue-autofluorescence images via deep learning," *Nature Biomedical Engineering*, vol. 3, no. 6, pp. 466-477, 2019.

[33] J. T. Springenberg, "Unsupervised and Semi-supervised Learning with Categorical Generative Adversarial Networks," *arXiv e-prints*, 2015.

[34] A. Odena, "Semi-Supervised Learning with Generative Adversarial Networks," *arXiv e-prints*, 2016.

[35] P. Shen *et al.*, "Conditional Generative Adversarial Nets Classifier for Spoken Language Identification," in *INTERSPEECH*, 2017, pp. 2814-2818.

[36] A. L. Goldberger *et al.*, "PhysioBank, PhysioToolkit, and PhysioNet: components of a new research resource for complex physiologic signals," *Circulation*, vol. 101, no. 23, pp. E215-20, 2000.

[37] G. B. Moody, and R. G. Mark, "The impact of the MIT-BIH Arrhythmia Database," *IEEE Engineering in Medicine and Biology Magazine*, vol. 20, no. 3, pp. 45-50, 2001.

[38] A. ECAR, "Recommended practice for testing and reporting performance results of ventricular arrhythmia detection algorithms," *Association for the Advancement of Medical Instrumentation*, pp. 69, 1987.

[39] Y. H. Hu *et al.*, "A patient-adaptable ECG beat classifier using a mixture of experts approach," *IEEE Trans Biomed Eng*, vol. 44, no. 9, pp. 891-900, 1997.

[40] P. d. Chazal *et al.*, "Automatic classification of heartbeats using ECG morphology and heartbeat interval features," *IEEE Trans Biomed Eng*, vol. 51, no. 7, pp. 1196-206, 2004.

[41] W. Jiang, and S. G. Kong, "Block-Based Neural Networks for Personalized ECG Signal Classification," *IEEE Transactions on Neural Networks*, vol. 18, no. 6, pp. 1750-1761, 2007.

[42] Z. Zhang *et al.*, "Heartbeat classification using disease-specific feature selection," *Computers in Biology and Medicine*, vol. 46, pp. 79-89, 2014.

[43] S. Raj, and K. C. Ray, "Sparse representation of ECG signals for automated recognition of cardiac arrhythmias," *Expert Systems with Applications*, vol. 105, pp. 49-64, 2018.

[44] F. Chollet *et al.*, "R Interface to Keras," GitHub, 2017.

[45] S. Ioffe, and C. Szegedy, "Batch Normalization: Accelerating Deep Network Training by Reducing Internal Covariate Shift," *arXiv e-prints*, 2015.

[46] N. Srivastava *et al.*, "Dropout: a simple way to prevent neural networks from overfitting," *J. Mach. Learn. Res.*, vol. 15, no. 1, pp. 1929-1958, 2014.

[47] X. Mao *et al.*, "Least Squares Generative Adversarial Networks," *arXiv e-prints*, 2016.

[48] M. Arjovsky *et al.*, "Wasserstein GAN," *arXiv e-prints*, 2017.

[49] I. Gulrajani *et al.*, "Improved Training of Wasserstein GANs," *arXiv e-prints*, 2017.

[50] D. P. Kingma, and J. Ba, "Adam: A Method for Stochastic Optimization," *arXiv e-prints*, 2014.

[51] G. Garcia *et al.*, "Inter-Patient ECG Heartbeat Classification with Temporal VCG Optimized by PSO," *Scientific Reports*, vol. 7, no. 1, pp. 10543, 2017.